Supplementary Information

Monolithic carbon derived from biomass *via* zinc-assisted pyrolysis for lithium-sulfur batteries

Jiahao Huang,[‡a] Zongle Huang,[‡a] Chen Zhang,[‡a] Tianliang Hao,[a] Tao Wang,[a] Dingfei Deng,[a] Zhipeng Sun,[a] Yue Wang,[a] Chenyang Xu,[a] Jinjue Zeng,[*a] Shaochun Tang,[*a] Chaobo Huang,[b] Lijun Yang[c] and Xuebin Wang[*a]

[a] National Laboratory of Solid State Microstructures (NLSSM), Collaborative Innovation Center of Advanced Microstructures, Frontiers Science Center for Critical Earth Material Cycling, College of Engineering and Applied Sciences, Nanjing University, Nanjing 210093, China

[b] College of Chemical Engineering, Nanjing Forestry University, Nanjing 210037, China

[c] Key Laboratory of Mesoscopic Chemistry of Ministry of Education, School of Chemistry and Chemical Engineering, Nanjing University, Nanjing 210093, China

[‡] These authors contributed equally to this work.

[*] Corresponding authors.

E-mail addresses: zengjinjue@nju.edu.cn, tangsc@nju.edu.cn, wangxb@nju.edu.cn

Supplementary Materials and Methods

Synthesis of Li_2S_6 solution and Li_2S_8 electrolyte: Sulfur and Li_2S with a molar ratio of 5:1 were added to the mixture solution of DOL and DME with a volume ratio of 1:1, and the concentration of Li_2S_6 solution was controlled to be 0.2 M. The Li_2S_8 electrolyte was prepared by mixing sulfur and Li_2S with a molar ratio of 7:1 in the same solvent containing 1.0 M LiTFSI.

Li_2S nucleation tests: The cells were assembled by using ZRC and RC as working electrodes with a diameter of 12 mm, lithium metal as the counter electrode, and Celgard 2400 as the separator. 30 μL of 0.2 M Li_2S_8 electrolyte was added to the side of the working electrode and 30 μL of 1 M LiTFSI electrolyte to the other side, respectively. The cells were galvanostatically discharged to 2.06 V at 0.112 mA, and then potentiostatically at 2.05 V until the current went below 10^{-5} A. The precipitation capacity of Li_2S was calculated *via* Faraday's law.

Polysulfide diffusion test: ZRC and RC were ground into powder and mixed with PVDF in a mass ratio of 9:1 to make a slurry, which was uniformly filtered onto the separator to prepare a thin film composite. The film composite was placed in the middle of the device with Li_2S_6 solution added to one side and DOL/DME (*v*:*v* = 1:1) added to the other. In another test, ZRC and RC powders were directly added to a small vial containing Li_2S_6 electrolyte and left to stand for 12 h. The visual changes were recorded by digital cameras. The changes in solutions were characterized by UV-vis absorption spectroscopy.

Density functional theory (DFT) calculation: The theoretical calculations were performed using the Vienna *Ab initio* Simulation Package (VASP) framework. The Perdew-Burke-Ernzerhof (PBE) functional was employed to describe the electron interaction of exchange-correlation.

The cutoff energy of the plane wave basis was set to 500 eV, with energy and force convergence criteria set to 1×10^{-5} eV *per* atom and 1×10^{-2} eV $Å^{-1}$, respectively. The vacuum region of 20 Å was set to prevent interference between adjacent layers. A 3 × 3 × 1 Monkhorst-Pack sampling of *K*-point in the irreducible Brillouin zone was applied. The adsorption energy (ΔE_a) was calculated by equation (1).

$$\Delta E_a = E_{(polysulfide+carbon)} - E_{(polysulfide)} - E_{(carbon)} \quad (1)$$

where $E_{(polysulfide+carbon)}$, $E_{(polysulfide)}$, and $E_{(carbon)}$ were the energy of polysulfide molecules adsorbed on the carbon, the energy of isolated polysulfide molecules, and the energy of the carbon, respectively. The Gibbs free energy (ΔG) was calculated by equation (2).

$$\Delta G = \Delta E_a + \Delta E_{ZPE} - T\Delta S \quad (2)$$

where ΔE_a, ΔE_{ZPE}, and $T\Delta S$ are the adsorption energy, zero-point energy difference, and entropic contributions (T was set to 298.15 K), respectively. The Li_2S dissociation energy barriers on different substrates were calculated using the climbing-image nudged elastic band (CI-NEB) method to evaluate the delithiation reaction kinetics.

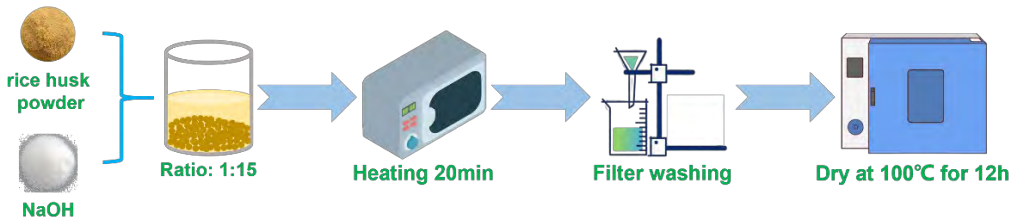

Figure S1. The procedure for treating rice husk powder with NaOH.

The application of HF is founded solely on a generic processing solution for silicon removal, and the following alternative solution can actually be used. NaOH is utilized in place of HF. Firstly, the waste stream from NaOH treatment is relatively manageable and safe to handle, primarily through neutralization, and exhibits a reduced environmental impact. More importantly, NaOH treatment can effectively remove lignin and hemicellulose from rice husk without degrading cellulose, leading to a significantly increase in the specific surface area and porosity of rice husk powder. NaOH serves as a pore regulator, and the derived rice husk-based porous carbon is characterized by a large specific surface area, uniform pore size, and narrow pore distribution. The following steps outline the procedure for treating rice husk with NaOH.

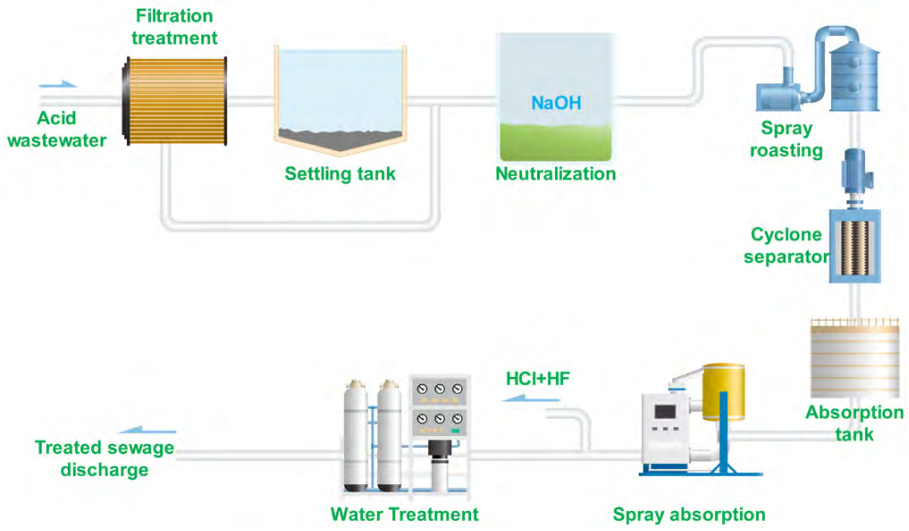

Figure S2. The procedures for recovery and treatment of acid-containing waste liquid.

The following solutions are provided for treating waste liquid generated by HCl and HF. i) Neutralization treatment: The waste liquid undergo neutralization to reduce acidity and facilitate subsequent treatment. Appropriate amount of sodium hydroxide or sodium carbonate can be added to the waste liquid to bring the pH value to neutral or near-neutral range. ii) Recycling through roasting: Neutralized waste liquids are processed using spray roasting techniques. The waste liquids undergo heating and decomposition, resulting the formation of hydrogen chloride gas and hydrofluoric acid gas. Both can enter the absorption tower to be absorbed by the scrubber water for the purpose of regeneration. iii) Post-processing and resource utilization: Further treatment of the remaining wastewater is required to comply with discharge standards. Various methods, including biological treatment and chemical precipitation, can effectively eliminate residual organic matter and inorganic salts from wastewater. iv) Resource recycling: The recycled hydrochloric acid and hydrofluoric acid can be reused in other industrial production processes to achieve resource recycling.

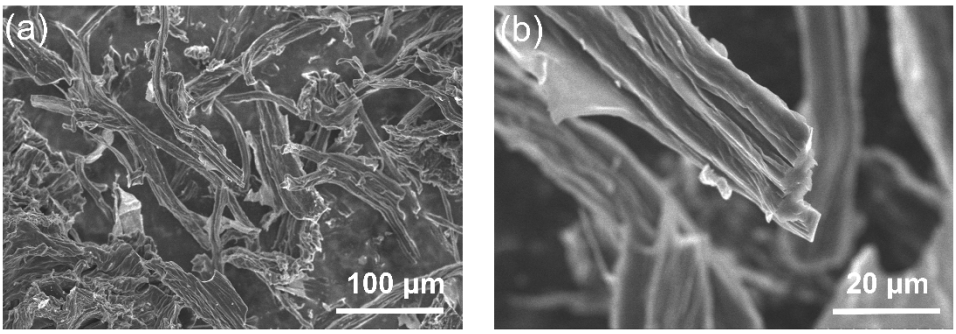

Figure S3. (a, b) SEM images of RC.

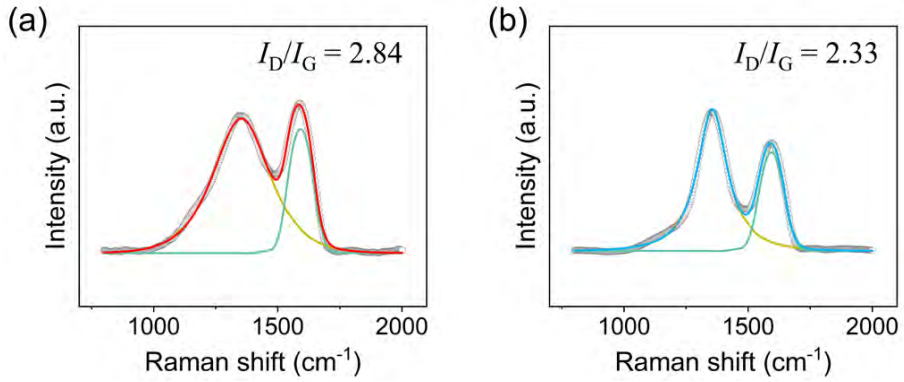

Figure S4. Peak fitting of Raman spectra.

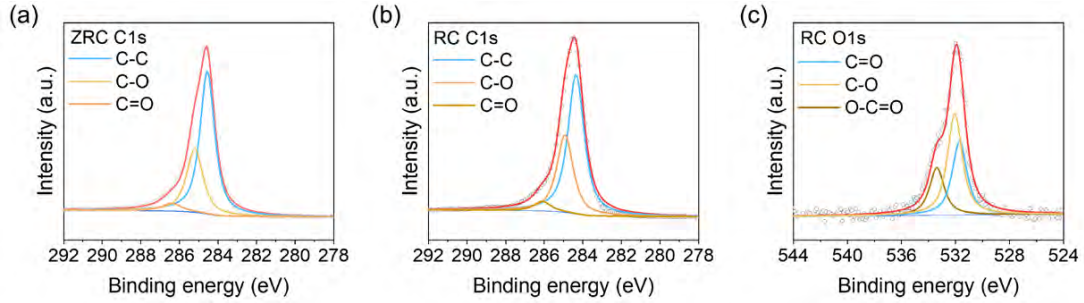

Figure S5. (a) High-resolution C 1s spectrum of ZRC. High-resolution (b) C 1s and (c) O 1s spectrum of RC.

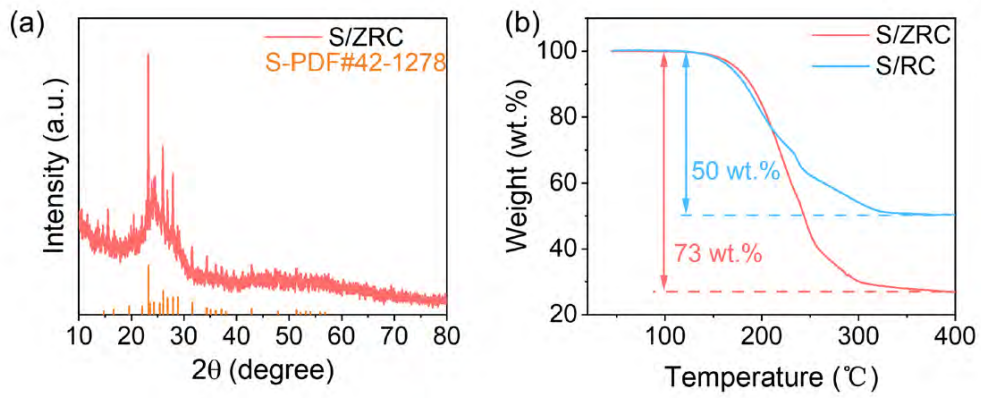

Figure S6. (a) XRD pattern of S/ZRC and the standard diffraction of S. (b) TGA curves of S/ZRC and S/RC.

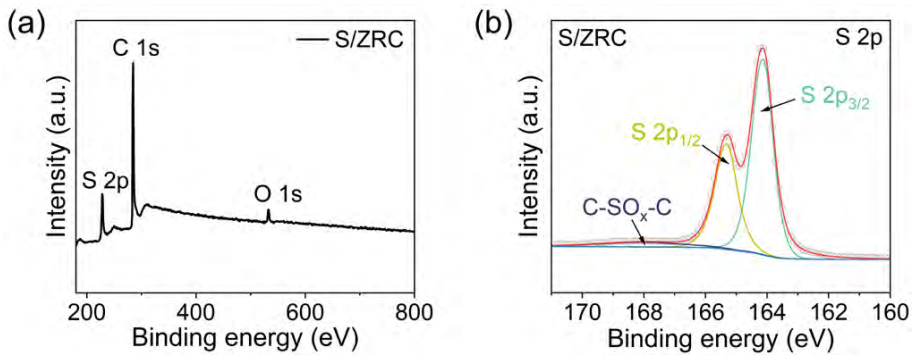

Figure S7. (a) XPS survey spectra of S/ZRC. (b) High-resolution S 2p spectra of S/ZRC.

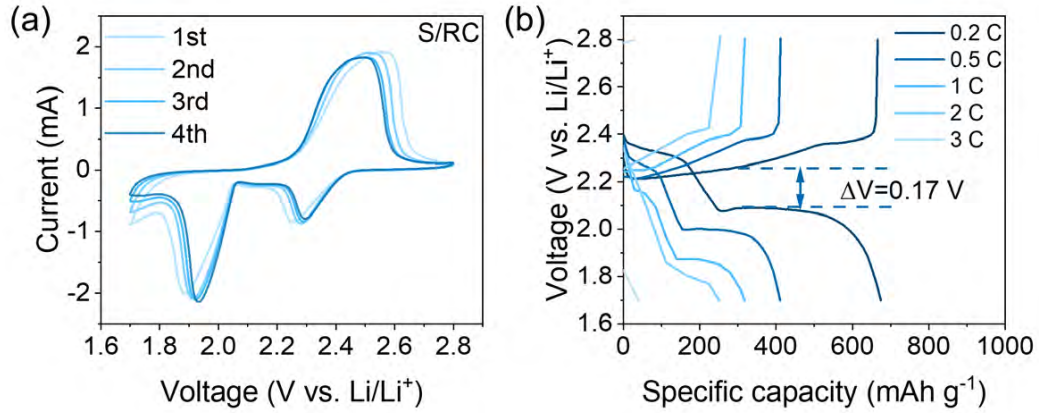

Figure S8. (a) CV curves of the initial four cycles for S/RC cathode. (b) GCD curves of S/RC cathode at different rates.

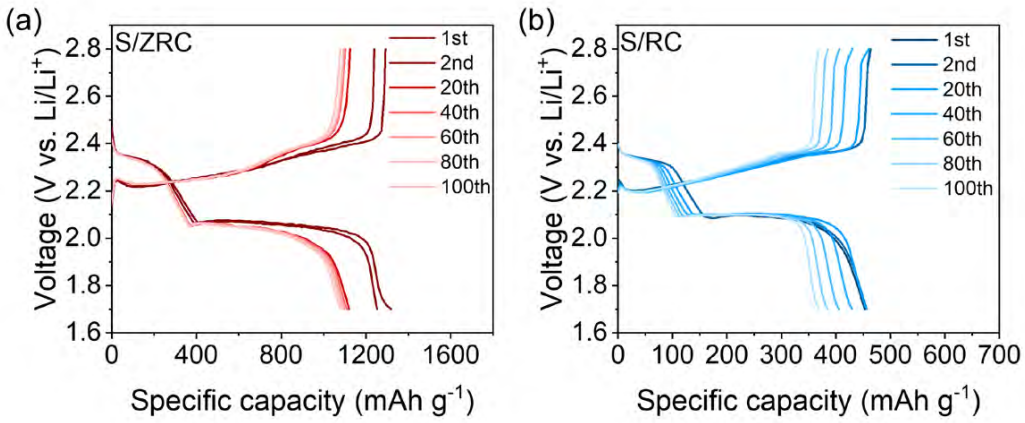

Figure S9. GCD curves at different cycle numbers: (a) S/ZRC and (b) S/RC cathodes.

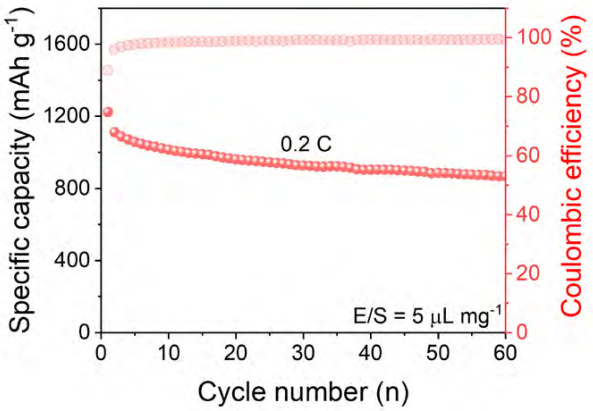

Figure S10. Cycling performance of S/ZRC in lean electrolyte of 5 μL mg^{-1}.

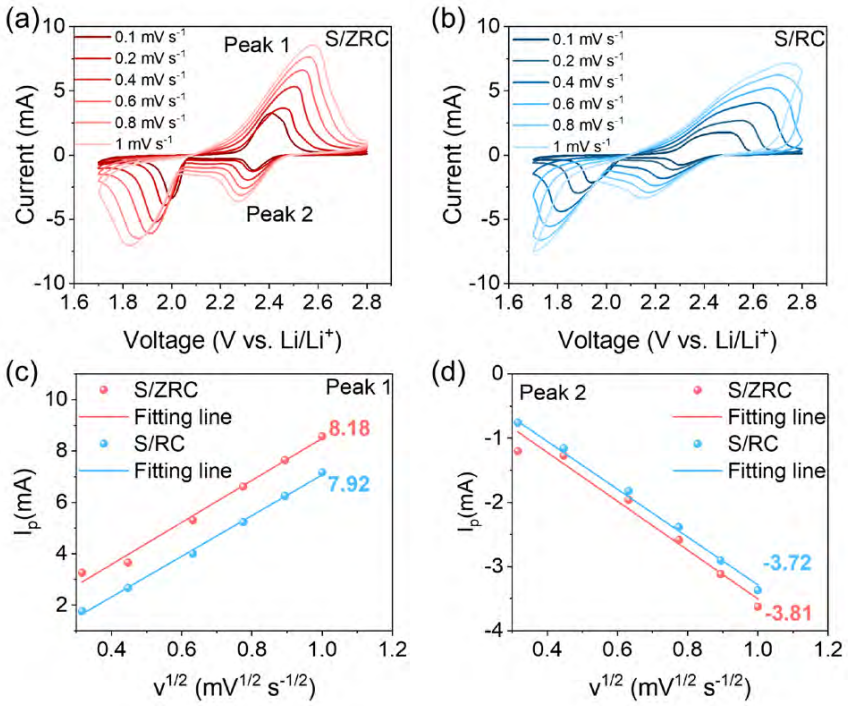

Figure S11. CV curves of (a) S/ZRC and (b) S/RC at different scan rates at 0.1-1.0 mV s^{-1}. Fitting of peak current values versus the square root of scan rates regarding (c) peak 1 and (d) peak 2.

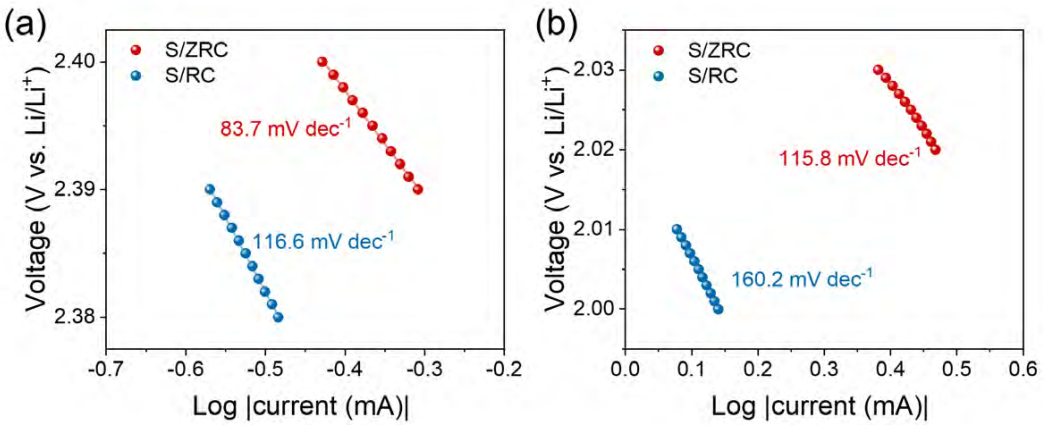

Figure S12. Tafel plots of different electrodes in the cathodic process. (a) The peak around at 2.4 V. (b) The peak around at 2.0 V.

Table S1. Comparison of carbon-supported composite cathodes for Li-S batteries.

Samples	Sulfur loading (wt.%)	Capacity at 1 C ($mAh\ g^{-1}$)	Rate ($mAh\ g^{-1}$)	Ref.
S/ZRC	73	850	721 at 3 C	This work
3DCF/S	90	762.8	601 at 2 C	[1]
NH_2-PLCNFs	78	786.2	597 at 2 C	[2]
S/PCNS	44	375.2	303 at 2 C	[3]
BCP/S	80	606	462 at 2 C	[4]
G/S/NRPF_5	58.7	783.8	645 at 5 C	[5]
3DCNF	63	691	433 at 5 C	[6]
NPCN/S	65.4	594	594 at 2 C	[7]
PI/CNT/CNT/S	70	600	350 at 2 C	[8]
S/CNT/G-50	67.39	715	545 at 3 C	[9]
S/NCNS/MWCNT	54	800	800 at 1 C	[10]
S/PCNFs	43.2	412	483 at 1 C	[11]
rGO/FPC/S	/	696	548 at 2 C	[12]
NG/S-CNT	60.6	655.9	450 at 2 C	[13]
S/PCNF/CNT	62	677.2	550 at 2 C	[14]
S/G/NPCFs	53	745.4	540 at 5 C	[15]
PCF/S	51	638	456 at 2 C	[16]
S-HNMC	53.3	600	595 at 3 C	[17]
NOPC/S	64.5	725.7	482.7 at 2 C	[18]
NSHPC	80	515	/	[19]
S/ACF	60	820	700 at 2 C	[20]

S/ONPC	47.6	331	613 at 0.2 C	[21]
S/OBC	58.5	561	665 at 0.5 C	[22]
PRC/Ni/S	76.1	777.1	573.5 at 5 C	[23]
S/NOPC-600	54.33	537	355 at 2 C	[24]
S/$LaNiO_3$	75	600	365.3 at 5 C	[25]
S/SG	73	301	118 at 2 C	[26]
LG/S	74	857	579 at 2 C	[27]
S@C/VN	78	673.6	370.3 at 3 C	[28]
S/CF	42.6	530	737 at 0.2 C	[29]
S/P-NCMO	75	793	657 at 3 C	[30]

Reference

[1] X. Liu, Z. Xiao, C. Lai, S. Zou, M. Zhang, K. Liu, Y. Yin, T. Liang and Z. Wu, *J. Mater. Sci. Technol.*, 2020, **48**, 84–91.

[2] M. Sun, X. Wang, Y. Li, Z. Zhao and J. Qiu, *Energy Environ. Mater.*, 2023, **6**, e12349.

[3] J. Guo, J. Zhang, F. Jiang, S. Zhao, Q. Su and G. Du, *Electrochim. Acta*, 2025, **176**, 853–860.

[4] L. Zhang, W. Zhao, S. Yuan, F. Jiang, X. Chen, Y. Yang, P. Ge, W. Sun and X. Ji, *J. Energy Chem.*, 2021, **60**, 531–545.

[5] J. Park, W. Choi, J. Yang, D. Kim, H. Gim and J. Lee, *Carbon*, 2021, **172**, 624–636.

[6] S. Feng, J. Song, S. Fu, C. Zhu, Q. Shi, M. Song, D. Du and Y. Li, *J. Mater. Chem. A*, 2017, **5**, 23737–23743.

[7] M. Xiang, Y. Wang, J. Wu, Y. Guo, H. Wu, Y. Zhang and H. Liu, *Electrochim. Acta*, 2017, **227**, 7–16.

[8] S. Deng, Q. Zhang, Q. Huang, D. Tang, P. Mei and Y. Yang, *Compos. Commun.*, 2022, **29**, 101019.

[9] M. Wei, H. Zhu, P. Zhai, L. An, H. Geng, S. Xu and T. Zhang, *Nanoscale Adv.*, 2022, **4**, 4809–4818.

[10] C. Hu, C. Kirk, J. Albero, F. Reinoso and M. Biggs, *J. Mater. Chem. A*, 2017, **5**, 19924–19933.

[11] R. Li, Y. Dai, W. Zhu, M. Xiao, Z. Dong, Z. Yu, H. Xiao and T. Yang, *Ionics*, 2022, **28**, 2155–2162.

[12] Y. Yan, Y. Yang, C. Fan, Y. Zou, Q. Deng, H. Liu, D. Brandell, R. Yang and Y. Xu, *ChemElectroChem*, 2022, **9**, e202200191.

[13] P. Zhai, J. Huang, L. Zhu, J. Shi, W. Zhu and Q. Zhang, *Carbon*, 2017, **111**, 493–501.

[14] Y. Zhang, Z. Zhang, S. Liu, G. Li and X. Gao, *ACS Appl. Mater. Interfaces*, 2018, **10**, 8749–

8757.

[15] X. Song, S. Wang, Y. Bao, G. Liu, W. Sun, L. Ding, H. Liu and H. Wang, *J. Mater. Chem. A*, 2017, **5**, 6832–6839.

[16] Q. Zhu, H. Deng, Q. Su, G. Du, Y. Yu, S. Ma and B. Xu, *Electrochim. Acta*, 2019, **293**, 19–24.

[17] Y. Qu, Z. Zhang, X. Zhang, G. Ren, Y. Lai, Y. Liu and J. Li, *Carbon*, 2015, **84**, 399–408.

[18] F. Chen, J. Yang, T. Bai, B. Long and X. Zhou, *Electrochimica Acta*, 2016, **192**, 99–109.

[19] S. Jiang, M. Chen, X. Wang, Y. Zhang, C. Huang, Y. Zhang and Y. Wang, *Chemical Engineering Journal*, 2019, **355**, 478–486.

[20] J. Zhang, J. Xiang, Z. Dong, Y. Liu, Y. Wu, C. Xu and G. Du, *Electrochimica Acta*, 2014, **116**, 146–151.

[21] Y. Zhao, L. Wang, L. Huang, M. Y. Maximov, M. Jin, Y. Zhang, X. Wang and G. Zhou, *Nanomaterials*, 2017, **7**, 402.

[22] Y. Yan, M. Shi, Y. Wei, C. Zhao, M. Carnie, R. Yang and Y. Xu, *Journal of Alloys and Compounds*, 2018, **738**, 16–24.

[23] Y. Zhong, X. Xia, S. Deng, J. Zhan, R. Fang, Y. Xia, X. Wang, Q. Zhang and J. Tu, *Advanced Energy Materials*, 2018, **8**, 1701110.

[24] J. Ren, Y. Zhou, H. Wu, F. Xie, C. Xu and D. Lin, *Journal of Energy Chemistry*, 2019, **30**, 121–131.

[25] S. Hong, Q. Li, J. Li, L. Jin, L. Zhu, X. Meng, Y. Che, Z. Yang, Z. Zhang, J. Yu and J. Cai, *ACS Applied Materials & Interfaces*, 2024, **16**, 35063–35073.

[26] R. Forde, A. T. S. C. Brandão, D. Bowman, S. State, R. Costa, L.-B. Enache, M. Enachescu, C. M. Pereira, K. M. Ryan, H. Geaney and D. McNulty, *Bioresource Technology*, 2024, **406**, 131065.

[27] Y. Luo, F. Xu, L. Sun, Y. Xia, Y. Yao, Y. Guan, S. Fang, H. Hu, C. Zhang, R. Cheng, Y. Zhu, Q.

Shao, Y. Zou, B. Shi and R. Li, *Journal of Energy Storage*, 2024, **85**, 111067.

[28] R. Liu, L. He, Y. Liu, J. Wu, W. Zhu, K. Xie, W. Liu, X. Lin, L. Shi, S. Wang, X. Feng and Y. Ma, *Materials Chemistry and Physics*, 2024, **315**, 129045.

[29] Q. Tang, L. Wang, Z. Xue, C. Li, D. Lv, N. Zhang and K. Zhu, *ACS Applied Nano Materials*, 2025, **8**, 863–870.

[30] R. Gao, L.-Y. Tian, T. Wang, H.-J. Li, P. Chen, T.-Y. Yan and X.-P. Gao, *ACS Applied Materials & Interfaces*, 2024, **16**, 21943–21952.